Carpathian Journal of Earth and Environmental Sciences, August 2020, Vol. 15, No. 2, p. 461 – 470; Doi:10.26471/cjees/2020/015/145

THE USE OF AERIAL LIDAR AND STRUCTURE FROM MOTION (SFM) PHOTOGRAMMETRY DATA IN ANALYZING MICROTOPOGRAPHIC CHANGES ON HIKING TRAILS ON THE EXAMPLE OF KIELCE (POLAND)

Piotr Tomasz KOPYŚĆ

Jan Kochanowski University, Institute of Geography and Environmental Sciences Kielce
Adress: Uniwersytecka 7, 25-406 Kielce, Poland E-mail: piotr.kopysc@phd.ujk.edu.pl

Abstract: This paper is an attempt to compare digital elevation models obtained through aerial LiDAR and Structure from Motion (SfM) techniques in order to record microtopographic changes on hiking trails within a 4-year period. For this purpose, two separate test fields were selected based on topographic change potential in the form of a near 0-degree trail slope alignment angle. The test fields are located in a forested area of Kielce city on a "red" hiking trail. The findings show that the microtopographic changes caused by natural processes and human use of the trail can be recorded by applying the techniques mentioned above. A comparison between the DEMs was done with the help of 24 cross-section transects and a raster calculation. Calculated values of absolute differences in hight ranged from 0.01 ± 0.01 m to 0.09 ± 0.01 m for a first test field and from 0 ± 0.01 m to 0.13 ± 0.01 m for second test field. Although the results have been presented, many challenges, such as error estimation, DEM creation obstacles, and accuracy difference, have been overcome to do so. Therefore, this approach must be used with caution. Potential improvements to the comparing techniques can be employed for further research to match the specific needs of an analysis of hiking trails.

Keywords: Hiking Trails, LiDAR, SFM, DEM, Raster calculation, Kielce

1. INTRODUCTION

With ideas such as smart cities more and more data are becoming accessible for managers and communities as a whole. These data have their uses, such as community projects, investments, spatial planning and remote measurements. Kielce, located in the central region of Świętokrzyskie Voivodeship (Poland), invested in three major aerial LiDAR projects in the last decade, in the years 2011, 2016, and 2019. Point clouds obtained through this aerial scanning present opportunities for a new insight into existing problems (Dwivedi et al., 2015) One such problem is the state and management of the hiking trail networks in the city's recreational areas. These networks are susceptible to anthropogenic and natural degradation factors. Many of which are related to topography such as slope, land cover and terrain roughness, or to use such as the type and amount of human use (Wilson & Seney, 1994, Leung & Marion, 1996, Olive & Marion, 2009, Gołaszewski et al., 2010, Tomczyk & Ewertowski, 2013). The importance of this problem and its impact on the environment as a whole has been widely accepted in numerous works (Cole, 1993, Leung & Marion, 1999, Dixon et al., 2004, Hill & Pickering, 2006, Tomczyk & Ewertowski, 2011). In the past, scientists proposed original approaches to assess changes on tourist routes (Cole 1983, Leung & Marion, 1999, Marion & Olive, 2006). Now, with the use of geostatistics and spatial analysis, over-time topographic changes on hiking trails can be determined by the creation of multiple high-resolution digital elevation models (DEMs) representing different periods of time (Perroy et al., 2010). Aerial laser scanning is a costly way of obtaining data and time intervals between every scan are counted in years, therefore the reconstruction of the microtopographic changes must be supported by an additional method of data gathering. Structure from Motion is a low-cost technique that allows for gathering high accuracy data for smaller areas (Kaiser et al., 2014), which in its effectiveness and accuracy can be a solid alternative to terrestrial laser scanning (Nouwakpo et al., 2016). Therefore, this technique can fill the gaps in aerial laser scanning resulting in an enhanced view of the

issue and a reconstruction of dynamic processes. This study is an attempt to compare the results of the digital elevation model created from the aerial LiDAR point clouds and its counterpart obtained through the photogrammetry SfM technique on an example of small research test fields located on the hiking trail network in Kielce.

1.1 Goal of the research

The main goal of this paper is to measure the level of soil degradation and record trail surface changes over 4-years period with the use of digital elevation models obtained through aerial LiDAR and SfM photogrammetry on hiking trails in forested areas of Kielce city. Realization of this goal allowed answering the research question: Are common signs of degradation such as trail widening and erosion detectable this way? Additional justification of this goal comes down to the popularization of the SfM technique for hiking trail management as a low-cost method of data gathering and a supplement for aerial LiDAR data.

2. METHODS

2.1 Study area

The city of Kielce is located in the western part of the Holy Cross Mountains. Surrounded by the forested mountain ranges, Kielce presents recreation opportunities for its inhabitants and tourists. The city's borders stretch from the south-west "Zgórskie" and southern "Posłowicko-Dymińskie" mountain ranges with the highest peak mount Telegraf 408 m.a.s.l. to the northern "Masłowskie" mountain range. On the western side, the "Kadzielniańskie" mountain range is contained within the city's borders, while on the eastern side the "Szydłówkowskie" hills mark the eastern reach of the city.

The river "Silnica" flows through the city and marks its valley within the city border in the south-west direction. The area of Kielce is known locally for a large number of protected areas such as nature reserves and landscape protection parks, which take up to 25 percent of its total area. The potential for tourism development can be seen in increasing usage of tourist accommodation over the years 2015-2020

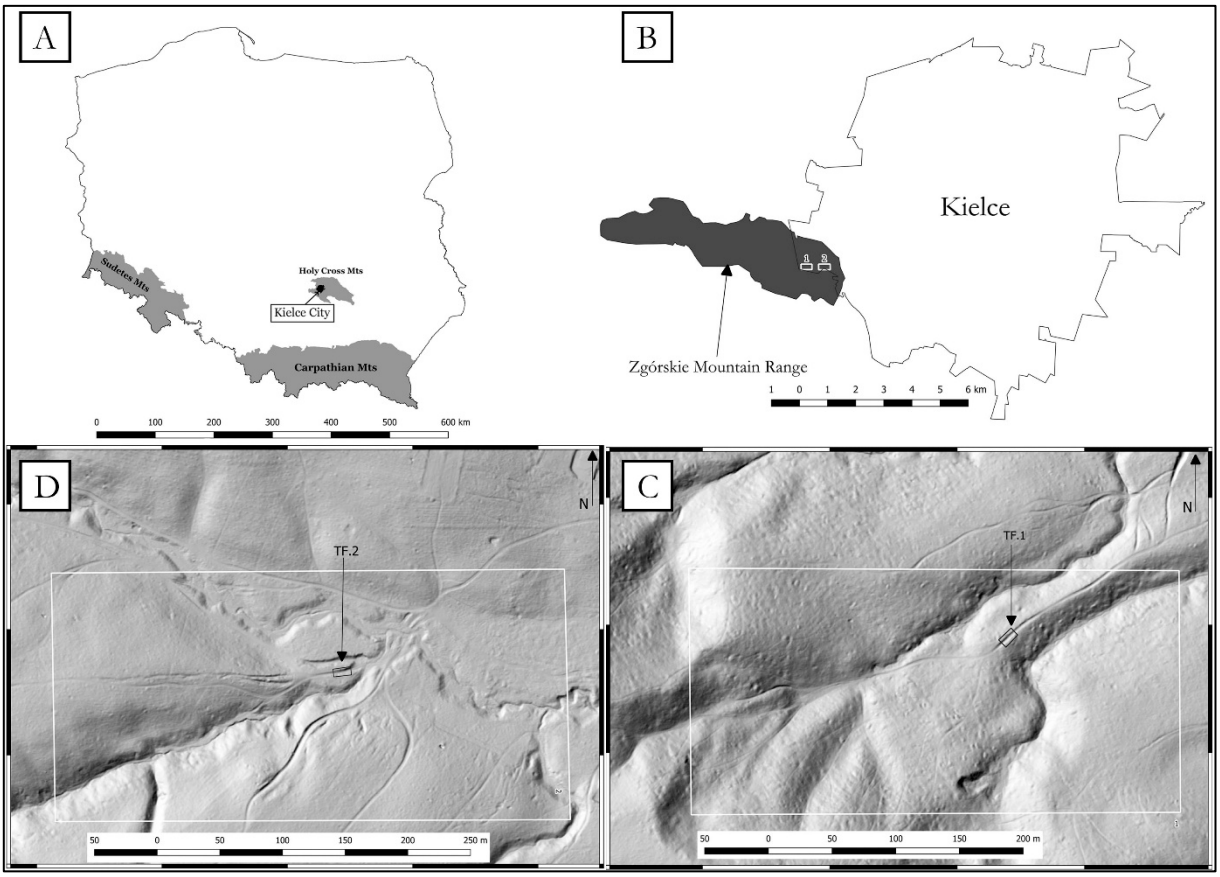

Figure 1. Study area. A) Location of Kielce city in Poland, B) Location of the "Zgórskie" mountain range in relation to Kielce, number 1, and 2 represents the areas where the research test fields are located. C) Research test field area and Test field 1 (TF1) location. D) Research test field area and Test field 2 (TF2) location.

and in the growing number of international tourists. The hiking trail network in Kielce city has a length of over 145 km and a density of 1.35 km per square kilometer, with different types of use including pedestrian, biking, and horse trails. For comparison, the hiking trails network density in the mountainous Tatra National Park is 1.3 km per square kilometer (Kozyra, 2013). This national park was visited by 3.3 m tourists in 2015 (Kruczek, 2016). In addition to formal hiking trails in Kielce, there are also informal forest paths that present a similar level of use. It is important to mention that in Kielce tourist trails, besides their original role, also play a transportation role in forestry. Heavy vehicle tracks on the hiking trail network were recorded during the fieldwork for this study. The signs of the movement of the vehicles are related to increasing degradation which manifests itself by increased soil compaction and rill erosion. A similar problem was indicated in studies from other areas in Poland (Tomczyk & Ewertowski, 2011, Kiszka, 2010). This study focuses on a forested tourist trails segment located on the "Zgórskie" mountain range in the south-western side of the city, (Fig. 1B) marked as a red trail, named after Sylvester Kowalczewski, a famous Polish touring enthusiast and a geography teacher. The trail was designed for pedestrian use. To realize the goal of this study, two separate research test fields were chosen based on field surveys performed by the author and a trail slope alignment angle indicator (Marion & Olive, 2006). Both test fields have a length of 10 m and a width that varies and depends on the trail width, thus ranging from 2.55 m to 4.3 m. Test field 1 is located higher, 303 m.a.s.l. on a mountain ridge. Both sides of the trail are forested, the slope of the landform where the field is located reaches 8 degrees into the northeast direction. The trail width in the test field varies from 3.14 m to 4.3 m in its widest part. The maximum incision recorded in the trail area reaches 95 cm. The trail surface shows the presence of exposed tree roots on its sides. The trail slope alignment angle for this field is close to 0 degrees, which results in an eroded U-shaped trail surface (Fig. 2A). On the side of the main trail path, a new path emerges as trampling is visible. This indicates that the original, now deeply incised trail is hard to walk on. Tourists and recreationists chose to walk on its side which resulted in a new track. Test field 2 is located lower in the mountain range, closer to the city, 265 m.a.s.l., with a direct neighborhood of forest stream. The land cover of this field has a higher plant density than that of TF1 and the slope of TF2 is equal to 7.97 degrees. The trail width in the test field varies from 2.55 m to 3.53 m in its widest part. The maximum incision recorded in the trail area reaches 128 cm. TF2 is directed in the Northeast. Both the land slope and trail have this direction which results in a 0-degree trail slope alignment angle. The shape of Test field 2 (Fig. 2B) reminds one of a gully with roots exposed on its sides rather than in the center. With much denser vegetation and high incision, tourists are forced to use the trail in order to move forward into the mountains, therefore no new paths are created.

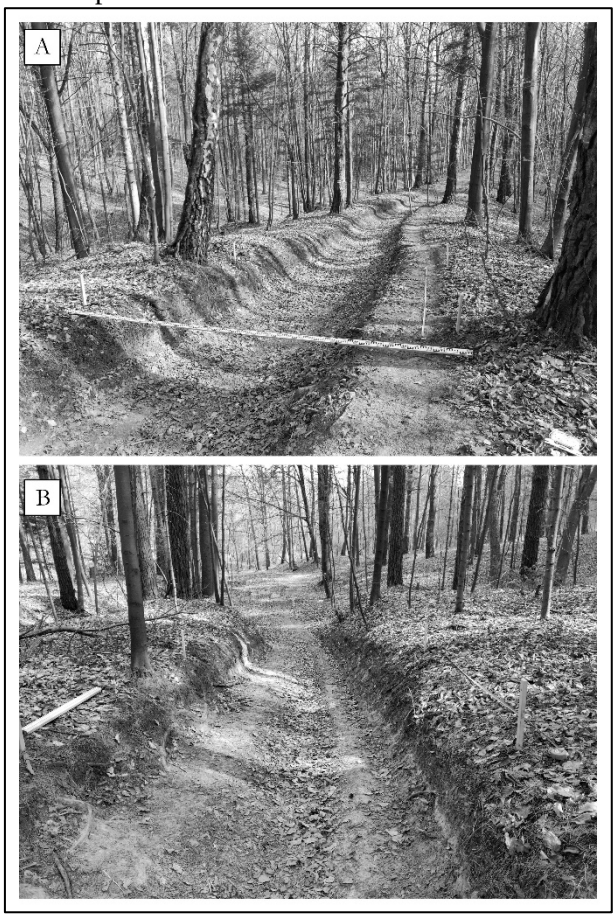

Figure 2. Picture of the first (A) and second (B) test field.

2.2 Equipment, data sources and software

The main data source used for conducting this research were 2016 and 2019 aerial LiDAR point clouds of Kielce with a point density of 24 points per square meter. For this research, data was obtained from the Kielce city department by the Jan Kochanowski University for scientific needs. Other data such as SfM point clouds and GIS indicators were collected and measured by the author during the field survey which was performed in March 2020. During the field survey, field morphometry data was collected with the use of basic instruments such as measuring tape, a laser measuring tool, and a measuring pole. In order to perform measurements and the installation of ground control points (GCPs), both test fields were segmented into 3 rectangular chunks (Fig. 3). Each field had a total of 8 GCPs, half

of them were placed on the right side and the other half on the left. The GCP position was recorded with a GPS receiver (Trimble GeoXH 2008 series) and its position was then manually corrected based on a distance and azimuth measurement to the nearby trees and in relation of the trees to each other. The reference point for the GCP location correction was 2019 aerial LiDAR point cloud data where the GCP location was corrected to match a specific point of longitude, latitude, and altitude. For a GCP, an SfM marker in the form of a wooden stake of 45 cm in length was used. A sign was painted on it in order to avoid mistakes in post-processing. To perform Structure from Motion, technique specific equipment and software were prepared. For this study, a 48 Mpix Sony IMX586 Exmor RS camera placed inside of a Xiaomi 9T Pro smartphone was used to capture images. The camera was placed on a stabilizing stick in order to avoid the loss of focus during camera movement. The camera focus was fixed to the geometry center of every chunk of the test field to avoid changes in the lens focus. (Fig. 3). Pictures were taken during cloudy weather to avoid lighting changes. Three main types of software were used to conduct the research. QGIS 3.1.4 served as a GIS desktop environment to perform analysis and store data within shape files. This software played an important role in the creation of cross-sections (transects) for comparison between specific DEMs. SAGA GIS was used to process raw LiDAR data that were turned into DEMs of the test fields. It provided tools necessary for that process, such as segmentation of point clouds, DEM filtering, a closing gaps tool, and a grid calculator used for DEM calculations and corrections. Finally, Agisoft Metashape Pro 1.6 served as the main tool to create, edit, and process the DEMs obtained through SfM photogrammetry.

2.3 DEM creation procedure

The Digital Elevation Models (DEMs) had a special creation procedure that was repeated for both test fields. First began the preparation phase in which the aerial LiDAR point cloud data was imported into SAGA GIS. In order to create a DEM with a very high resolution, only the test field point cloud had to be extracted from the original cloud. This was achieved by the extraction tool with the use of a shape file representing each field. After extracting a box of points representing the ground and trees, another segmentation took place with the use of the same tool. This time, the extraction rule was the height value, points that were over 10 cm above the ground were removed leaving only points representing the ground. This allowed for the creation of a raw Grid DEM. With the use of the DEM filter tool in SAGA GIS, based on the information provided by Vosselman

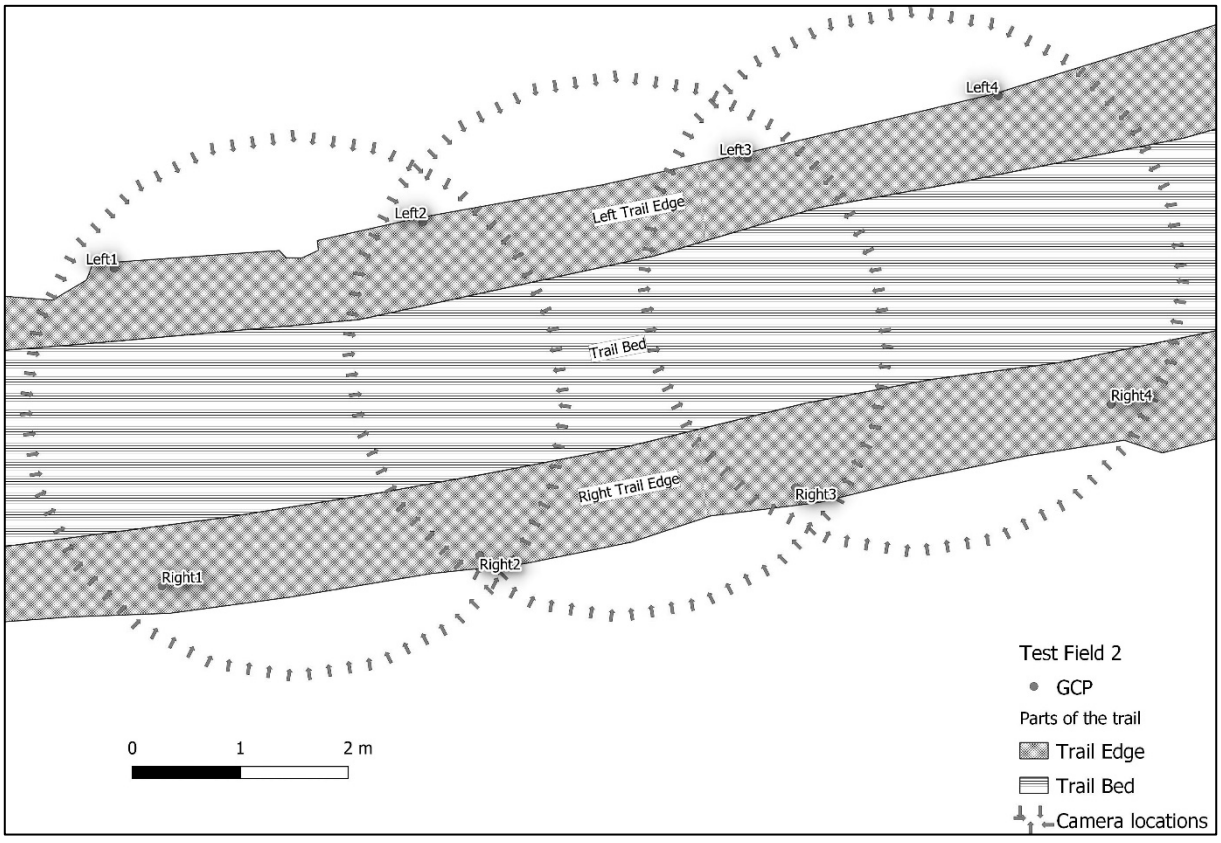

Figure 3. SfM field procedure with the GCP and camera locations, an example of Test field 2.

(2000), both grids could have been pruned of leftover vegetation data leaving only the bare earth model. Because this process created new empty data cells in the Grid, a "close gap with spline" tool was used to fill the gaps and complete the DEM. With the use of B-Spline interpolation, a 10 cm resolution of a bare earth DEM was achieved (Fig. 4B, 4D). The next step was to import the created DEM into the QGIS environment together with measurement data for the GCP. With the DEM as a reference point and with the help of the data (GPS, length, and azimuth to the nearest trees) a GCP shape file was created. This file was then used in SfM photogrammetry as a reference point for markers. In order to produce the DEM from pictures taken during a field survey in March 2020, 184 pictures with the resolution of 8000x6000 px for Test field 1 and 202 pictures with the same quality for Test field 2 were split into 3 chunks and imported into Agisoft Metashape Pro. Then the LiDAR 2016 DEM created in the SAGA GIS and GCP shape file was also imported into Agisoft. The first step included putting the GCP as a marker on the pictures.

After that the set of photos was aligned with settings as follows: Accuracy - High, Reference preselection - Subsequential, with an advanced setting staying as default. With tie points ready, a dense cloud point was generated using these settings: Quality - Medium, Filtering mode - Aggressive. Finally, all 3 chunks were connected based on matching points, which resulted in a full dense point cloud for the entire field. In the end, a 3 mm resolution DEM was created (Fig. 4A, 4C) which was then imported into the QGIS environment for comparison with the aerial LiDAR DEM The comparison between the LiDAR 2016 DEM and the 2020 SfM DEM was achieved in two ways, first by comparing cross-section transects (24) and the absolute values of the hiking trail width and the maximum incision. The second comparison was done with a raster calculator tool and a subtraction between them. For this study, the horizontal and vertical error value was estimated based on previous research in which the same methods were applied (Hladik & Alber, 2012, Nouwakpo et al., 2016, Kolzenburg et al., 2016).

Although the root mean square error for the SfM method can be very small, for example a 0.3 mm achieved in previous studies (Nouwakpo et al., 2016, Vinci et al., 2017) for this study a 5 cm horizontal and 1 cm vertical RMSE was applied, which was based on research conducted by Perroy et al., (2010) with the use of similar aerial LiDAR data.

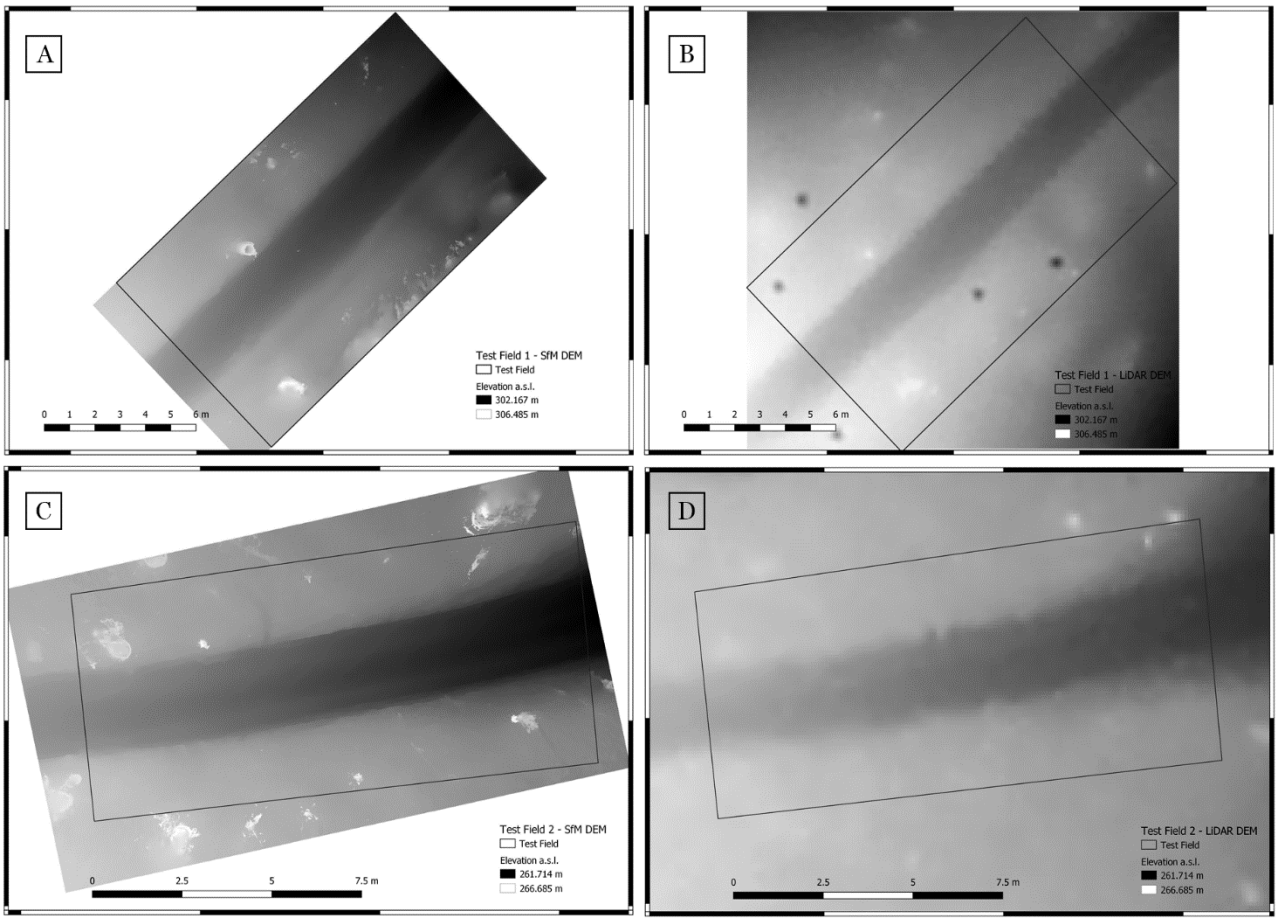

Figure 4. Digital elevation models for Test field 1 created with the use SfM (A) of and aerial LiDAR (B). Test field 2 is represented by DEMs made with SfM (C) and aerial LiDAR (D)

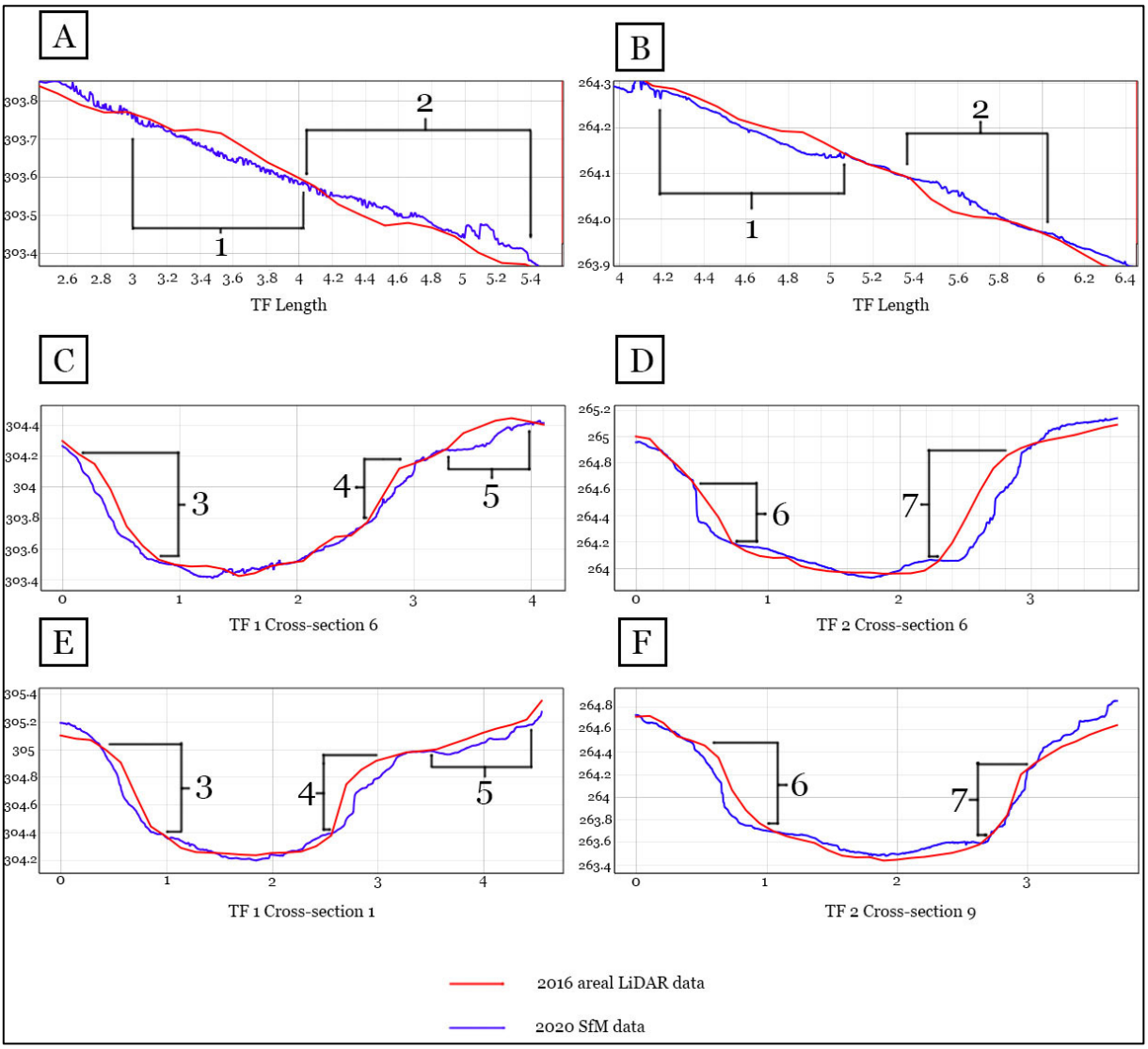

Figure 5. Road transects comparison (A, B): detection of cases of micro-erosion (1) and micro-deposition (2) on both TF1 (A) and TF2 (B). (C, E): comparison between TF1 cross-sections; the trail widening is represented by the change in the left (3) and right (4) edge of the trail. Additional path in Test field 1; height changes are visible in (C5) and (E5). Test field 2: the trail widening is represented by cross-sections (D, F) where (6) represents changes on the left and (7) on the right side.

3. RESULTS

3.1 DEM description

With the use of given means and procedures, the gathered data resulted in the creation of DEMs that represented specific points in time. Aerial LiDAR point density turned out to be smaller on the ground than expected which was caused by the trees' canopy cover where some points were stuck on the leaves. SfM dataset did not have such issue. Although, it had other issues of a regional loss of accuracy. Most of the model (central part) where the GCPs were located, matched the aerial LiDAR DEM very well. Cross-section transect lines showed minimal deformation of the SfM DEM in comparison to the LiDAR DEM. However, closer to the edges of the SfM DEM grid, larger and larger deviations were recorded. These border areas were omitted for measurements.

3.2 Transects comparison

The first way of comparing the DEMs was to calculate differences in the height of the trail surfaces. The results of cross-section transect measurements indicate that even small changes that occurred throughout the 4-year period can be recorded (Fig. 5). Results from Test fields 1 and 2 show that only small changes occurred on the trail bed, including micro-erosion and micro-deposition of the soil (Fig. 5A, 5B).

It was confirmed during the field survey that the soil compaction on these test fields was very high, therefore the trail bed itself was resistible to greater changes in such a short period. In the case of trail edges,

much greater changes were recorded in the form of trail widening in transects 1, 7, 11, and 12 for Test field 1 and transects 5, 6, and 9 for Test field 2. This widening is caused by the movement on the trail and sediment-water flow down the slope (Fig. 5C, 5D, 5E, 5F). In close proximity to trees, the trail edges remained more stable; this is the result of roots that hold trail edge structure together. The existence and exposure of roots were confirmed during the field survey. As an additional result in the case of Test field 1, more changes occurred on the smaller, extra path next to the trail. TF1 transects show that a barely visible additional track in 2016 became a fully formed incised and 60-80 cm wide path in 2020. The greatest change occurred on transects 4 and 6 where height differences on the newly created path next to the hiking trail reached 16 ± 1 cm (Fig. 5C); changes on that path can be seen in most of the TF1 transects. That would indicate higher pedestrian movement causing trampling and vegetation cover loss since the path is still too small for vehicles.

3.3 DEM calculation comparison

The second way of making the comparison employed for this study was to calculate the difference in the height of each cell between both the aerial LiDAR and SfM DEMs. With the use of the QGIS raster calculator, aerial LiDAR DEM height values were subtracted from SfM height values for both test fields (Fig. 6). The results confirm the findings of the transects comparison and uncover new facts. Trail bed changes on TF1 can be seen on the entire length. The height changes on the trail bed were unchanged or negative, which may be related to a higher position above sea level and a location of an accumulation spot lower in the mountain range. TF2, however, showed different results where a trail bed height change was negative at a higher altitude and positive at a lower altitude. This positive change may be directly related to the accumulation of eroded

Table 1. Transects measurements of width and incision values and absolute differences together with an error.

TF 1 Transects Results						
Transect	2016 LiDAR Width (m)	2020 SfM Width (m)	Absolute Difference ± Error value (m)	2016 LiDAR Maximum Incision (m)	2020 SfM Maximum Incision (m)	Absolute Difference ± Error value (m)
1	3.47	3.68	0.21 ± 0.05	0.84	0.87	0.03 ± 0.01
2	3.67	3.97	0.3 ± 0.05	0.89	0.9	0.01 ± 0.01
3	3.65	3.73	0.08 ± 0.05	0.85	0.89	0.04 ± 0.01
4	3.15	3.49	0.34 ± 0.05	0.77	0.78	0.01 ± 0.01
5	3.71	3.91	0.2 ± 0,05	0.82	0.84	0.02 ± 0.01
6	3.14	3.57	0.43 ± 0.05	0.88	0.89	0.01 ± 0.01
7	3.72	3.58	0.14 ± 0.05	0.94	0.95	0.01 ± 0.01
8	3.52	3.57	0.05 ± 0,05	0.82	0.88	0.06 ± 0.01
9	3.37	3.41	0.03 ± 0.05	0.71	0.78	0.07 ± 0.01
10	3.6	3.66	0.06 ± 0,05	0.73	0.81	0.08 ± 0.01
11	3.43	3.64	0.22 ± 0.05	0.67	0.76	0.09 ± 0.01
12	3.14	3.35	0.21 ± 0.05	0.69	0.7	0.01 ± 0.01
TF 2 Transects Results						
Transect	2016 LiDAR Width (m)	2020 SfM Width (m)	Absolute Difference ± Error value (m)	2016 LiDAR Maximum Incision (m)	2020 SfM Maximum Incision (m)	Absolute Difference ± Error value (m)
1	2.55	2.59	0.03 ± 0.05	0.86	0.93	0.07 ± 0.01
2	2.96	2.85	0.11 ± 0.05	0.79	0.79	0 ± 0.01
3	2.76	2.78	0.02 ± 0.05	0.86	0.84	0.03 ± 0.01
4	2.81	2.92	0.12 ± 0.05	0.9	0.97	0.07 ± 0.01
5	2.72	2.9	0.18 ± 0.05	1.01	1.04	0.03 ± 0.01
6	2.55	2.78	0.22 ± 0.05	1.04	1.03	0.01 ± 0.01
7	2.9	2.97	0.07 ± 0.05	1.08	1.13	0.06 ± 0.01
8	3.11	3.2	0.09 ± 0.05	1.05	1.04	0.01 ± 0.01
9	3.16	3.34	0.18 ± 0.05	1.28	1.24	0.04 ± 0.01
10	3.31	3.25	0.06 ± 0.05	1.26	1.13	0.13 ± 0.01
11	3.38	3.4	0.02 ± 0.05	1.11	1.07	0.04 ± 0.01
12	3.41	3.53	0.12 ± 0.05	1.12	1.01	0.11 ± 0.01

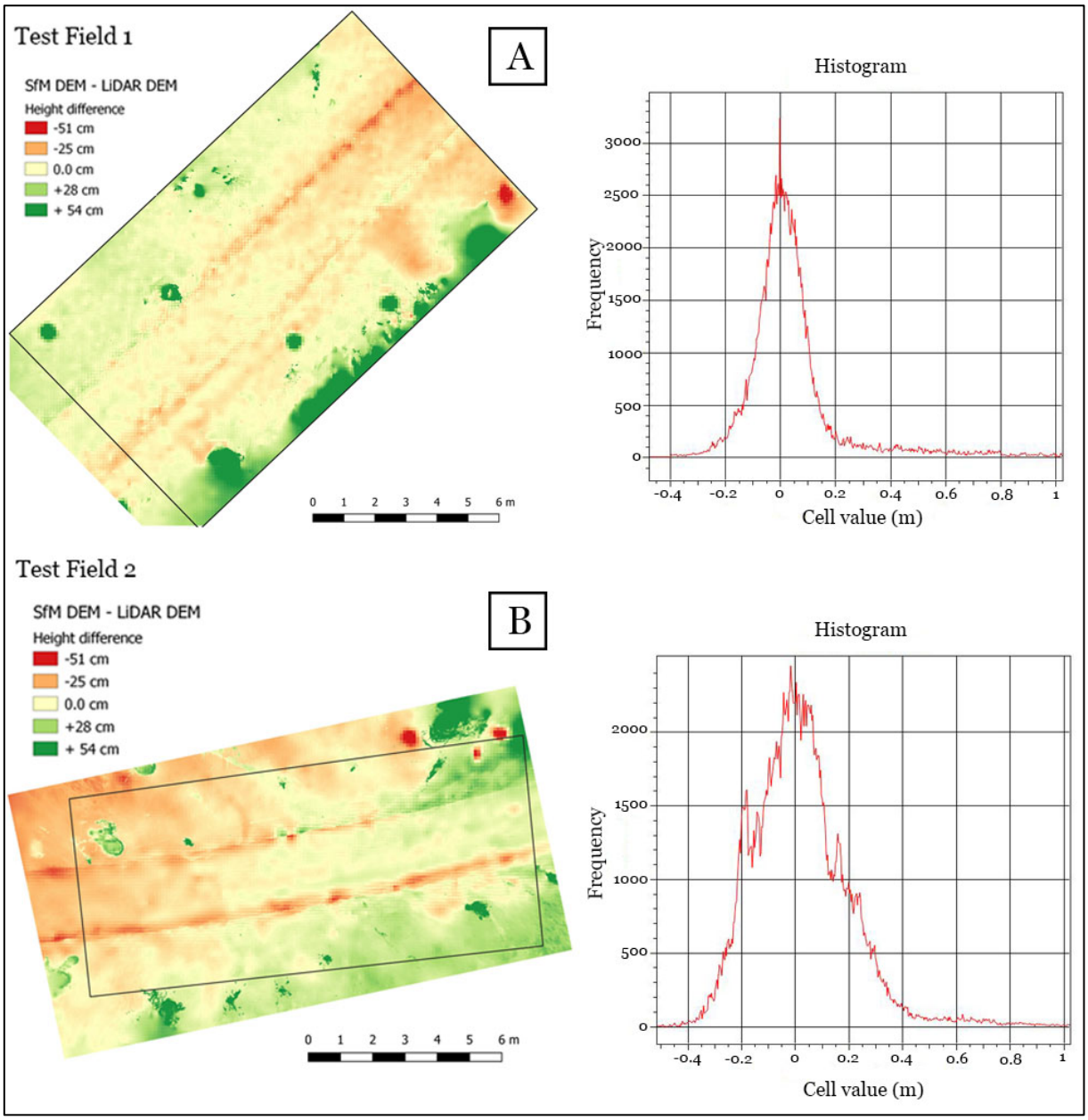

Figure 6. The result of raster substraction of the 2016 aerial LiDAR DEM for the 2020 SfM model for TF1 (A) and TF2 (B). The histograms represent a frequency of cell values within a raster calculation for each field.

material. Within a calculation grid, another trend can be seen. Trail edges, as has been indicated by the transects comparison, are subject to erosion, which results in trail widening. The widening is stronger on edges without trees and weaker in their presence. Slope direction is also connected to trail edge erosion; a sedimentary flow of water most likely erodes the edge that stands on its way. That can be seen in Test field 1 where slope direction slightly changes in the middle (Fig. 6A). This results in stronger erosion on the right side and then the left side from the top. Test field 2, however, has the slope directed into the stream within its neighborhood which, in turn, erodes the right side edge more than the left side (Fig. 6B).

4. DISCUSSION

4.1 Results comparison

This study found that absolute hight values derived from DEMs calculations were similar to the one presented in Kaiser et al., (2014). However, the difference of 4-year period research to a one-year period in Kaiser et al,. (2014) uncovers that much more drastic changes occurred in their study area. The reason for this might be that soil erosion rates on trails are uneven and very diverse for different areas and conditions (Salesa & Cerda 2020). Or that changes on hiking trails do not occur in a linear trend but rather dynamic and continuous erosive and accumulative

events as presented by Tomczyk et al., (2016). Both Test fields in this study were deeply incised from 0.69 m to 0.96 m for a TF1 and from 0.86 m to 1.28 m for a TF2. Such deep trail incision was studied before by Johnson & Smith (1983) in the form of off-road vehicles (ORV) impact on soil loss. These scientists found a yearly lowering rate of 140 mm per year. In this study, the lowering rate appears much smaller which can be explained by different types of the trail (pedestrian vs ORV) and different amount of use. Finally, this study mean erosion rates estimated from two test fields (0.85 ± 1 cm per year for TF1 and -0.11 ± 1 cm per year from TF 2) are similar to other studies conducted by Bodoque et al., (2017) in Spanish Pyrenees (0.3 ± 0.15 cm to 0.9 ± 0.43 cm per year). Erosion rates presented here are smaller than studies performed by Tomczyk & Ewertowski (2013) in Gorce National Park in Poland (1.6 to 2.5 cm per year).

4.2 Research limitation

Aerial LiDAR and SfM techniques were compared in the past years in different scenarios, for example, in volcanology (Kolzenburg et al., 2016) or geomorphology (Grohmann et al., 2020) and separately (Perroy et al., 2010, Kaiser et al., 2014). All of these mentioned studies had challenges and obstacles to overcome in order to compare both aerial LiDAR and SfM. In this study, such obstacles also existed. Although point clouds are a good source of data in creating digital elevation models, sometimes they prove very challenging to generate a DEM in the correct shape. To achieve a good comparison similar point density clouds would be preferred. This was not the case in this study. Aerial LiDAR scanning data was pushed to its limits in order to achieve a 10 cm resolution DEM. As stated by Eagleston & Marion (2020) higher resolution then 50 cm is preferred to obtain correct values. SfM could easily generate a 3mm resolution DEM with an even better possible resolution. This obstacle of resoultion diference was overcome with an application of aerial LiDAR mean square root error as a primary accuracy scale. At the top of this, other challenges were recorded specifically for each point cloud. One such challenge for the aerial LiDAR point cloud were "underground" false points which had an effect on the final shape of the DEM. This issue was resolved through the use of segmentation and manual extraction of these points. Since default filtering tools had trouble with filtering this data from underground, out of the point cloud, this manual procedure of cleaning was performed only for a hiking trail structure. This way the "underground" false points had no effect on the measurement and overall results. Apart from the issues of aerial LiDAR, there were also two significant issues with the SfM technique. The first one of them was the loss of accuracy in the test field borders. Areas located too far away from the GCPs were subject to deformation. Because of that, in deformed places, the SfM model did not match the aerial LiDAR model. These areas had to be omitted for this study. A similar problem had been mentioned in other studies, i.e. it was claimed that there was a loss of accuracy in the larger SfM models (Kolzenburg et al., 2016). The second significant issue in regard to the SfM technique was the existence of vegetation cover in the point cloud obtained from the test field. This obstacle does change the height of the ground and the overall shape of the DEM. A similar obstacle was noted by Nouwakpo et al., (2016) which was resolved in the development of a special filtering algorithm. In order to avoid possible errors and misinterpretation for this study and with the inability to apply filtering algorithms, vegetation cover points were manually removed from the point cloud of the hiking trails within the test field, with the exception of big trees. It is important to understand that these studies were conducted within limited self-funding. Therefore there are ways to improve the results, increase the accuracy and minimize error. For example, the use of a real-time kinematic station and a higher accuracy GPS receiver could result in better GCPs georeference. On the ground, a manual camera could be replaced by an unmanned aerial vehicle. Finally, different and more flexible software programs could be used to increase quality.

5. CONCLUSION

On the basis of the results of the study it can be concluded that both aerial LiDAR and SfM techniques can be used together in order to obtain a high-resolution comparison of microtopographic changes on hiking trails. This comparison allowed for the detection of common signs of degradation, such as trail widening. Calculated values of absolute differences in hight ranged from 0.01 ± 0.01 m to 0.09 ± 0.01 m for a first test field and from 0 ± 0.01 m to 0.13 ± 0.01 m for second test field. Although this method is not superior in accuracy compared to terrestrial laser scanning, it does open a possibility to deploy the easy to use, cheap SfM technique and to make a comparison with already existing aerial LiDAR data. Although the comparison is possible on hiking trails, more research is required for accuracy improvements and wider applications.

REFERENCES

Bodoque, J.M., Ballesteros-Cánovas, J.A., Rubiales, J.M., Perucha, M.A., Nadal-Romero, E. & Stoffel, M., 2017. *Quantifying soil erosion from hiking trail in a protected natural area in the Spanish Pyrenees.* Land Degradation & Development 28, 2255–2267.

Cole, D.N., 1983. *Assessing and monitoring backcountry trail conditions.* Research Paper INT-303. USDA Forest Service, Intermountain Forest and Range Experiment Station, Ogden, UT**.**

Cole, D.N., 1993. *Minimizing conflict between recreation and nature conservation* In D. Smith and P. Hellmund (eds.) Ecology of greenways: design and function of linear conservation areas. University of Minnesota Press, Minneapolis, 105-122.

Dixon, G., Hawes, M. & Mcpherson, G., 2004. *Monitoring and modelling walking track in pacts in the Tasmanian Wilderness World Heritage Area.* Journal of Environmental Managment 71. 305-320.

Dwivedi, M., Uniyal, A. & Mohan, R., 2015. *New Horizons in Planning Smart Cities using LiDAR.* Technology International Journal of Applied remote sensing and GIS 2, 40-50.

Eagleston, H. & Marion J.L., 2020. *Application of airborne LiDAR and GIS in modeling trail erosion along Appalachian Trail in New Hampshire, USA.* Landscape and Urban Planning 198 (2020).

Grohmann, H.C., Garcia, G.P.B., Affonso, A.A. & Albuquerque, R.W., 2020. *Dune migration and volume change from airborne LiDAR, terrestrial LiDAR and Structure from Motion-Multi View Stereo.* Computers & Geosciences 143.

Gołaszewski, M., Rojan, E. & Tsermegas, I., 2010. *Wpływ wybranych elementów środowiska przyrodniczego na stan szlaków turystycznych w Dolinie Pięciu Stawów Polskich.* In: Z. Krzan (ed.) Nauka a zarządzanie obszarem Tatr i ich otoczeniem 3, 29 – 35.

Hill, W. & Pickering, C. M., 2006. *Vegetation associated with different walking track types in the Kosciuszko alpine area*. Journal of Environmental Management 78, 24–34.

Hladik, C. & Alber, M 2012. *Accuracy assasment and correction of LIDAR-derived salt marsh digital elevation model.* Remote Sensing of Environment 121, 224–235.

Johnson, C.W. & Smith, J.P., 1983. *Soil loss caused by off-road vehicle use on steep slopes*. Transactions of the ASAE 26 (2), 402-405.

Kaiser, A., Neugirg, F., Rock, G., Müller, C., Haas, F., Ries, J. & Schmidt, J., 2014. *Small-Scale Surface Reconstruction and Volume Calculation of Soil Erosion in Complex Moroccan Gully Morphology Using Structure from Motion.* Remote Sensing 6, 7050-7080.

Kiszka, K., 2010. *Antropologiczne i naturalne uszkodzenia szlaków turystycznych.* Pieniny – Przyroda i Człowiek, 11, 157–169.

Kolzenburg, S., Favalli, M., Fornaciai, A., Isola, I., Harris, A.J.L., Nannipieri, L. & Giordano, D., 2016. *Rapid Updating and Improvement of Airborne LIDAR DEMs Through Ground-Based SfM 3-D Modeling of Volcanic Features.* IEEE Transactions On Geoscience And Remote Sensing 54,11, 6687 – 6699.

Kozyra, M., 2013. *Turystyka w górskich przygranicznych parkach narodowych w Europie.* Studia i Materiały CEPL w Rogowie 37,4, 177 – 183.

Kruczek, Z., 2016. *Frekwencja w atrakcjach turystycznych.* Polska Organizacja Turystyczna, Kraków-Warszawa, 94.

Leung, Y.F. & Marion, J.L., 1996. *Trail degradation as influenced by environmental factors: A state-of-the-knowledge review*. Journal of Soil and Water Conservation, 130-136.

Leung, Y.F. & Marion, J.L., 1999. *Assessing trail conditions in protected areas: application of a problem assessment method in Great Smoky Mountains National Park.* U.S.A. Environmental Conservation 26,4, 270–279.

Marion, J.L. & Olive, N.D., 2006. *Assessing and understanding trail degradation: results from big south fork national river and recreational area.* Research/Resources Management Report. USDI National Park Service, Big South Fork National River and Recreation Area, Onieda, TN.

Nouwakpo, S.K., Weltz, M.A. & McGwire, K., 2016. *Assessing the performance of structure from-motion photogrammetry and terrestrial LiDAR for reconstructing soil surface microtopography of naturally vegetated plots.* Earth Surface Processes and Landforms 41,13, 308-322 https://doi.org/10.1002/esp.3787

Olive, N.D. & Marion, J.L., 2009. *The influence of use-related, environmental, and managerial factors on soil loss from recreational trails.* Journal of Environmental Management 90, 1483–1493.

Perroy, R.L., Bookhagen, B., Asner, G.P. & Chadwick, O.A., 2010. *Comparison of gully erosion estimates using airborne and ground-based LiDAR on Santa Cruz Island, California.* Geomorfology 118, 288–300.

Salesa, D. & Cerda, A., 2020. *Soil erosion on mountain trails as a consequence of recreational activities. A comprehensive review of the scientific literature.* Journal of Environmental Management 271.

Tomczyk, A. & Ewertowski, M., 2011. *Degradation of recreational trails, Gorce National Park, Poland.* Journal of Maps 7, 507-518.

Tomczyk, A. & Ewertowski, M., 2013. *Planning of recreational trails in protected areas: Application of regression tree analysis and geographic information systems.* Applied Geography 40, 129–139

Tomczyk, A., White, P. & Ewertowski, M., 2016. *Effects of extreme natural events on the provision of ecosystem services in a mountain environment: The importance of trail design in delivering system resilience and ecosystem service co-benefits.* Journal of Environmental Management Volume 166, 156-167.

Vinci, A., Todisco, F., Brigante, R., Mannocchi F. & Radicioni, F., 2017. *A smartphone camera for the structure from motion reconstruction for soil surface variations and soil loss due to erosion.* Hydrology Research 48.3, 675-685.

Vosselman, G., 2000. *Slope based filtering of laser altimetry data.* IAPRS Journal of Photogrammetry and Remote Sensing 33,B3, 935-942.

Wilson, J.P. & Seney J.P., 1994 *Erosional Impact of Hikers, Horses, Motorcycles, and Off-Road Bicycles on Mpuntain Trails in Montana.* Mountain Research and Development 14. 77-88.

Received at: 26. 07. 2020
Revised at: 19. 08. 2020
Accepted for publication at: 17. 08. 2020
Published online at: 27. 08. 2020